Geoid
Journal of Geodesy and Geomatics

Geoid Vol. 21, No. 1, 2026, 102-116

P-ISSN: 1858-2281; E-ISSN: 2442-3998

Hydrogeochemistry and Genetic Fluids of the Non-Volcanic Geothermal System, Hot Spring in Tehoru District, Maluku Province, Indonesia

Yusuf Mehdi Khairi Toisuta*[1], Agus Didit Haryanto[1], Johanes Hutabarat[1]
[1] Department of Applied Geology, Faculty of Geological Engineering, Universitas Padjadjaran, Sumedang, Indonesia
*Corresponding author: yusuf17003@mail.unpad.ac.id

Received: 7 March 2026; Revised: 28 May 2026; Accepted: 2 June 2026; Published: 21 June 2026

Abstract: Maluku is one of the provinces in Indonesia with non-volcanic geothermal potential, as it is geographically located at the intersection of three active tectonic plates, the Eurasian, Pacific, and Indo-Australian. This supports the emergence of geothermal manifestations without volcanic activity. Tehoru is one of many areas with non-volcanic geothermal potential in Indonesia, located in the province of Maluku, Central Maluku Regency, Tehoru District. In this area, geothermal phenomena such as hot springs, mud pools, and fumaroles have been discovered. Based on anion-cation hydrogeochemical analysis and supported by the results of stable isotope analysis of $\delta^{18}O$ and $\delta^{2}H$, this research examines 4 samples of hot springs and 1 sample of a cold spring. Overall, these samples originate from heated meteoritic water, and the fluid interacts with rocks before reaching the surface as phreatic water. APTHR-2 appears in a state of full equilibrium, APTHR-1 and APTHR-3 appear in a state of partial equilibrium, while APTHR-4 and ADTHR-1 appear on the surface in a state of immature waters. The estimated reservoir temperature ranges from 161 to 194°C, indicating that the Tehoru geothermal system is a medium-enthalpy geothermal system. This is supported by the lithological conditions in the study area, which consist of metamorphic and altered rocks. Based on these analysis results, it can be confirmed that there is no volcanic activity in the Tehoru Geothermal Area, Maluku, Indonesia. The type of geothermal system in Tehoru is assumed to be a fractured system or heat sweep system.

Keywords : Hydrogeochemistry ,Geothermometry, Nonvolcanic, Indonesia.

How to cite: Yusuf, .M.K.T., Agus, D.T., & Hutabarat, J. (2026). Hydrogeochemistry and Genetic Fluids of the Non-Volcanic Geothermal System, Hot Spring in Tehoru District, Maluku Province, Indonesia. *Geoid 21(1) pp 102-116.*

Introduction

Geologically, Indonesia is very complex because it is situated at the intersection of three major tectonic plates, known as the Triple Junction: the Eurasian Plate, the Indo-Australian Plate, and the Pacific Plate (Rochayati, 2025 ; Fahira et al, 2025 ; Verstappen, 2010). The convergence of these plates plays a crucial role in the formation of volcanoes, which are sources of geothermal energy in Indonesia. The emergence of geothermal sources worldwide is largely associated with both active and inactive volcanoes. Each region in Indonesia has a different geothermal system and unique characteristics. The geothermal system in Indonesia also depends on parameters such as temperature, depth, and geological conditions (Santia et al., 2021).

Geothermal resources in Indonesia can be categorized as either volcanic or non-volcanic (Arrofi et al., 2022). Volcanic geothermal resources are found along the volcanic belt, which stretches from the islands of Sumatra, Java, Bali, the Nusa Tenggara Timur Islands, and Sulawesi to the Maluku Islands. Meanwhile, non-volcanic geothermal resources are located on the islands of Kalimantan, Bangka Belitung, Sulawesi, and Papua (Mulki et al., 2021).

There are 136 identified non-volcanic geothermal systems in Indonesia, accounting for approximately 38% of the total locations. The size of geothermal resources in non-volcanic environments is 4035 MWe, consisting of speculative resources of 2473 MWe, hypothetical resources of 607 MWe, and reserves of 955 MWe. The potential compared to total resources is 16% (Ministry of Energy and Mineral Resources of Indonesia, 2019).

Non-volcanic geothermal energy is one of the untapped or underdeveloped potentials in Indonesia's renewable energy sector (Kumalasari et al., 2020). This system is commonly found in areas that do not have active volcanic activity but have geological conditions that allow heat transfer from the earth's interior to the surface through mechanisms such as faults, fractures, and conduction from hot rocks at depth (Fink et al., 2021). The province of Maluku is one of the areas that has geothermal potential that is not directly related to volcanic activity (Pinning et al., 2023; Rezky & Zarkasyi 2010).

The research aims to determine the characteristics of the geothermal fluid and the origin of the geothermal fluid at the Tehoru, Central Maluku Regency, Maluku province, Indonesia, using hydrogeochemical and isotope data.

Administratively, the research location, namely the Tehoru geothermal area, is located in the Tehoru District, Central Maluku Regency, Maluku Province. Geographically, the research area is located in the southern part of Seram Island, in the Tehoru District, Central Maluku Regency, Maluku Province. The research location is approximately ±90 km from Masohi City, Central Maluku, and ±2 km from the village settlement to the forestry area. Tehoru Village is an area with fairly gentle terrain at an altitude of 0-300 meters above sea level and is located on the coast (Figure. 1).

In general, Maluku Province is divided into two physiographic units, namely the Outer Banda Arc and the Inner Banda Arc. Boano Island, Kelang Island, Seram Island, and Manipa Island belong to the Outer Banda Arc physiography, whereas Ambon Island and Haruku Island are part of the Inner Banda Arc, which is included within the Maluku Orogen (Tjokrosapoetro et al., 1993). The Tehoru area is located in the southern part of Seram Island. Physiographically, Seram Island belongs to the Outer Banda Arc, which is part of the Neogene imbrication belt (Koesomadinata, 2025; Carter et al., 1976)

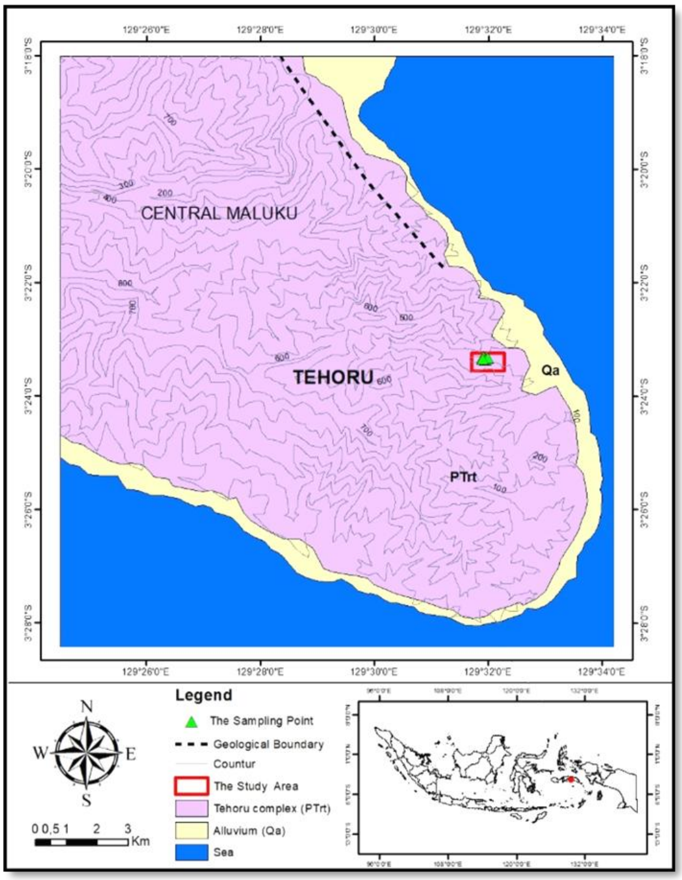

Figure 1. The Study Area on the Geological Map
(Part of Geological Map of the Masohi Quadrangle, Maluku, Indonesia, Thokrosapoetro, 1993).

The Tehoru region is part of the outer Banda Arc, which has no volcanoes (Syaiful, 2020). The Tehoru area is composed of the Tehoru Complex (PTrt) dating from the Permian to Triassic periods, which consists of metamorphic rocks with green schist, phyllite, sandstone, schist, psammitic, and calc-siliceous lithologies (Tjokrosapoetro et al., 1993; Figure 1). The geological structures found in the study area are folds and faults. The fold structure is an anticline with a relative axis oriented northwest-southeast, with a fault structure consisting of predominantly strike-slip faults, oblique faults, and normal faults. Strike-slip faults generally run west-east, northwest-southeast, and southwest-northeast. The oblique faults are oriented relatively northwest-southeast, while the normal faults are oriented relatively north-south (Directorate of Geothermal Energy, Ministry Energy of Indonesia, 2017).

Methodology

Non-volcanic geothermal systems generally have more limited surface manifestations than volcanic geothermal systems because they are not directly related to intense magmatic activity. The manifestations that appear are often only hot springs or hot water pools with scattered distribution and are rarely found on the earth's surface in non-volcanic geothermal systems. In the Tehoru geothermal system, the limited manifestation of hot springs resulted in only five research samples, covering all surface springs identified in the research area.In this study, geochemical and stable isotope analyses were conducted on several hot spring samples in the study area. Five samples consisting of four hot springs and one cold spring were collected and coded APTHR-1, APTHR-2, APTHR-3, APTHR-4, and ADTHR-1. The anion-cation content was analysed at the Center for Groundwater and Environmental Geology Laboratory. Stable isotopes ($\delta^{18}O$ and $\delta^{2}H$) were analysed at the Center for Coal and Geothermal Resources Laboratory. Both laboratories are part of the Ministry of Energy and Mineral Resources of Indonesia.

Based on laboratory analysis of chemical geothermal fluids, the results were applied to the ternary diagram (Giggenbach, 1988), Cl-SO_4-HCO_3, Cl/100-Li-B/4, and Na-K-Mg, Schohller diagram (Scohller, 1965), Stable isotopes $\delta^{18}O$ and $\delta^{2}H$ (Craig, 1961), as well as water geothermometer calculations (Giggenbach, 1988; Fournier, 1977). This was done to determine the characteristics or type and origin of geothermal fluids and to estimate the subsurface temperature for the geothermal system (Hochstein, 2000).

Water Sample Quality Assessment

Ion balance testing is conducted to evaluate the quality of fluid samples prior to further geochemical analysis. Laboratory analyses of water samples are considered valid and accurate when the ion balance value is less than 5% (Nicholshon, 1993; Powell and Cumming, 2010). According to Nicholson (1993), hot spring waters exhibiting an ion balance greater than 5% are strongly influenced by the fluid type and the geochemical processes affecting the system. The ion balance calculation is conducted by converting the concentrations of all charged ions from mg/kg into milliequivalent units (meq), followed by summing the total milliequivalents of cations and anions. The ion balance equation according to Nicholson (1993) is expressed as follows :

$$\%\ \text{Ion balance} = (\sum \text{Cation} - \sum \text{Anion}) / (\sum \text{Cation} + \sum \text{Anion}) \times 100\% \quad (1)$$

Ion balance analysis was carried out to assess the quality of the chemical data, using the procedures and acceptance criteria for geothermal water geochemistry proposed by Powell and Cumming (2010) (Table.1).

Table 1. Ion balance classification table according to Powell and CummingPowell and Cumming (2010).

Ion Balance Eror %	Data Quality Interpretation
<5%	Excellent
5-10%	Acceptable
>10%	Questionable / Possible analytical error

Determination of Water Type (Cl-SO_4-HCO_3 Ternary Diagram)

The type of hot water is determined based on the position of the chemical element ratio of Cl, SO_4 and HCO_3 on the ternary diagram. This analysis is carried out on each hot water source, and then, based on the position of the hot water, the type and cause will be determined (Giggenbach, 1988). The calculation of the relative ion content of Cl-SO_4-HCO_3 can be seen in the following equation:

$$S = [Cl] + [SO_4] + [HCO_3] \quad (2)$$

$$\% Cl = (100 [Cl]) /S \quad (3)$$
$$\% SO_4 = (100 [SO_4]) /S \quad (4)$$
$$\% HCO_3 = (100 [HCO_3]) /S \quad (5)$$

Analysis of Dissolved Substances

Soluble substances are categorized into geoindicators (reactive and reflective of equilibrium environments) and tracers (geochemically unreactive, difficult to react with, and traceable to their origin) (Giggenbach, 1991). The content of Cl, Li and B provides information on subsurface conditions due to their conservative nature (Giggenbach, 1988). Lithium (Li) acts as a tracer because it is resistant to secondary processes in showing the dissolution of the initial reservoir rock, while chloride (Cl) and boron (B) are conservative;boron concentrations tend to decline during the evolution of geothermal systems as a result of long-term heating and progressive fluid evaporation, while chloride (Cl) provides information related to fluid origin, hydrothermal flow pathways, and mixing processes within the geothermal system (Giggenbach, 1991; Nicholson, 1993). The calculation of relative ion content of Cl-Li-B can be seen in the following equation:

$$S = [Cl]/100 + [Li] + [B]/4 \quad (6)$$
$$\%B = (([B]/4)/S).100 \quad (7)$$
$$\%Li = ([Li]/S).100 \quad (8)$$
$$\%Cl = [Cl]/S \quad (9)$$

Water Maturity Analysis

The maturity of geothermal manifestations is determined through the relative content of Na, K and Mg elements using the Na-K-Mg ternary diagram (Giggenbach, 1988), in which Mg has a low concentration (0.01-0.1 ppm) at high temperatures, and an increase in its concentration is caused by dilution by surface water with high Mg content (Nicholson, 1993). The Na–K–Mg ternary diagram classifies geothermal fluids into three categories: Immature waters, Partial equilibrium, and Full equilibrium. Immature waters indicate that the geothermal fluid has mixed with near-surface fluids, particularly meteoric water. Partial equilibrium reflects a condition in which the fluid has undergone partial chemical equilibrium with reservoir rocks. In contrast, Full equilibrium indicates that the fluid has attained chemical equilibrium with the geothermal reservoir and originates directly from the reservoir with minimal influence from external processes or shallow fluid mixing (Giggenbach, 1988; Nicholson, 1993). The calculation of relative ion content of Na- K-Mg can be seen in the following equation:

$$S = ([Na]/1000) + ([K] / 100) + [Mg]^{1/2} \quad (10)$$
$$\% Na = (100([Na] / 1000))/S \quad (11)$$
$$\% Mg = (100 [Mg]^{1/2})/S \quad (12)$$
$$\%K = [K]/S \quad (13)$$

The Origin of Water

To determine the origin of the water, this study also approached isotopes $\delta^{18}O$ and $\delta^{2}H$. These two elements were used because they have stable properties and do not affect the interaction process between fluids rising to the surface and rocks (Murillo et al., 2015). This approach, using stable isotopes, can determine the origin of the hot spring fluid, as indicated by the ratio or content of the fluid isotopes themselves.

To obtain the results, the data from the stable isotope $\delta^{18}O$ and $\delta^{2}H$ laboratory analysis was then analyzed to determine the origin of the fluid, which was presented in the Relationship Between $\delta^{18}O$ and $\delta^{2}H$ Graph (Craig, 1961) by plotting the abundance values of the elements $\delta^{18}O$ and $\delta^{2}H$ against the Global Meteoric Water Line or Local Meteoric Water Line values The isotopic abundances of $\delta^{18}O$ and $\delta^{2}H$ were calculated using equations referenced to the Standard Mean Ocean Water (SMOW):

$$\delta^2H = (RH\ ^2HO_{sample} - RH\ ^2HO_{SMOW} / RH\ ^2HO_{SMOW}) \times 1000\ ^o/_{00} \quad (14)$$
$$\delta^{18}O = (RH_2{}^{18}O_{sample} - RH_2{}^{18}O_{SMOW}/RH_2{}^{18}O_{SMOW}) \times 1000^o/_{00} \quad (15)$$

Schoeller Diagram

Geochemical analysis is often used to understand water-rock interactions, sources of contamination, and characterization of water types based on major and minor ion content (Appelo & Postma, 2005). In groundwater and hot spring studies, identifying the content of elements such as Na, K, Ca, Mg, Cl, SO_4, and HCO_3 is important for assessing the origin of water and the geochemical processes that occur. The Schoeller diagram is a semi-logarithmic graphical representation used to compare the concentrations of major ions from several water samples simultaneously (Shah, 2021 ; Schoeller, 1965).

Water Geothermometer Analysis

Geochemical analysis of surface water is very important in calculating subsurface temperatures . Geothermometers are a method for estimating geothermal reservoir temperatures (Arnorsson et al, 1983). Geothermometers are often used in geothermal fields to determine reservoir temperatures. Geothermometers were developed with the primary purpose of estimating reservoir temperatures using water chemistry or isotopes. (D'Amore & Arnórsson, 2000).

Calculation of Na-K geothermometer using the equation :

a) $$[t^{o}C = \frac{1217}{\log\left(\frac{Na}{K}\right) + 1.483} - 273], \text{(Fournier, 1979)} \quad (16)$$

b) $$[t^{o}C = \frac{1390}{1.75 + \log\left(\frac{Na}{K}\right)} - 273], \text{(Giggenbach, 1988)} \quad (17)$$

Results and Discussion

Identification of the physical properties of hot springs through direct visual observation in the field of surface geothermal manifestations in the form of hot springs, warm water, and other surface manifestations such as solfataras, steaming ground, steam-heated water, and altered rocks. The emergence of geothermal manifestations on the surface is an indication of the existence of a hydrothermal system beneath the surface. In general, the physical properties of hot springs in the study area are clear (transparent), have varying temperatures and pH levels, and may or may not have a sulfur odor (Figure.2). Field observations of the physical properties of hot springs were conducted at five observation sites in Tehoru Village, Central Maluku Regency, Maluku Province (Table 2).

Table 2. Physical Characteristics of Springs in the Study Area

No	Sample Code	Coordinate	T Water	T Air	pH	Elevation (above sea level)	Description
1	APTHR-1	03°23’18” LS 129°31’54” BT	88.7 °C	31° C	7,9	158m	Slightly cloudy color, slight odor, produces bubbles, and Visible steam
2	APTHR-2	03°23’20.19”LS 129°31’54.70” BT	85° C	31° C	8.5	139m	Clear color, slight sulfur smell, emits bubbles, and Visible steam
3	APTHR-3	03°23’20” LS 129°31’54.72” BT	89 °C	32° C	8.4	136m	Clear color, slight sulfur smell, emits bubbles, and Visible steam
4	APTHR-4	03°23’21.88”LS 129°32’57.68” BT	67 °C	31° C	7.24	86m	Clear color, odorless, produces bubbles and Visible steam
5	ADTHR-1	03°23’20.31”LS 129°31’59.43” BT	27 °C	30 °C	7.62	81m	Clear color, odorless,

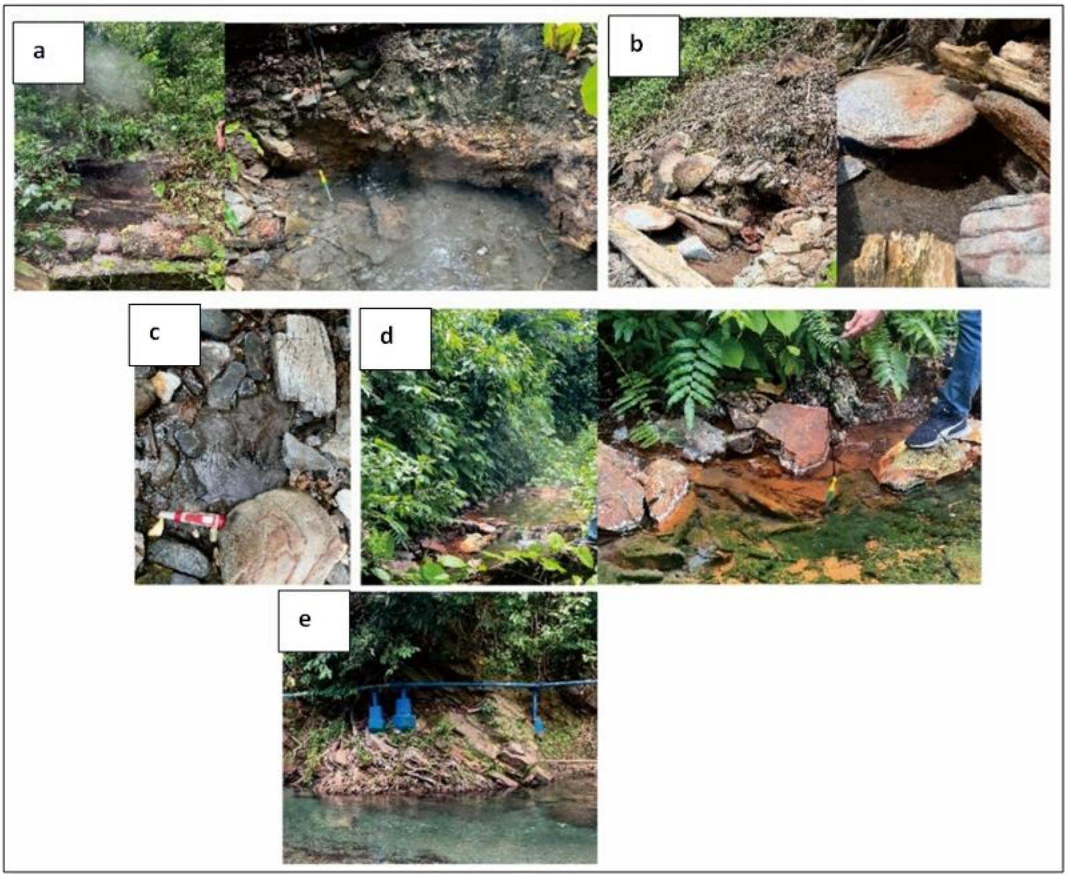

Figure 2. Hot and Cold Springs at Tehoru in Reasearch Area a) APTHR-1, b) APTHR-2, c) APTHR-3, d) APTHR-4, e) ADTHR-1

Laboratory Analysis Results (Water Sample Quality Assessment)

The characteristics of geothermal reservoir fluids are needed as one of the indicators in determining geothermal potential. Fluids from the four hot spring sources were then analyzed to determine the concentration of chemical elements contained therein. Test results from the Groundwater and Environmental Geology Center laboratory of the Indonesian Ministry of Energy and Mineral Resources show the chemical content found in the manifestation fluid (Table. 3).

Table 3. Results of Chemical Analysis of Spring

Anion-Cation Parameters, etc.	APTHR-1	APTHR-2	APTHR-3	APTHR-4	ADTHR-1
DHL µS/cm	4924,0	4981,0	4785,5	1416,0	217.4
pH	7,99	8,77	8,78	7,.23	7.62
Ca (Mg/L)	2,995	1,997	1,920	15,945	4,623
Mg (Mg/L)	1,800	0,0080	0,440	3,750	2,738
K (Mg/L)	59,480	59,710	61,840	17,320	2,313
Na (Mg/L)	1248,458	1241,373	1186,470	288,989	35,927
NH4 (Mg/L)	8,02	6,94	7,34	2,24	0,01

HCO3 (Mg/L)	2205,1	2211,1	2175,1	578,0	103,6
CO3 (Mg/L)	0,001	125,8	93,1	0,0001	0,0001
Cl (Mg/L)	449,932	452,642	4455,393	103,194	10,383
SO4 (Mg/L)	292,316	288,535	282,221	68,311	8,836
F (Mg/L)	5,262	5,299	5,177	1,598	0,190
SiO2 (Mg/L)	108,319	103,155	100,723	61,707	16,279
Al (Mg/L)	0,0644	0,0541	0,1110	<0,040	<0,040
As (Mg/L)	<0,0004	<0,0004	<0,0004	<0,0004	<0,0004
B (Mg/L)	13,838	15,845	15,018	3.52	0,344
Li (Mg/L)	1,360	1,400	1,320	0,335	0,030
Ion balance Equilibrium	1%	-3%	-3%	1%	-2%

The results show that the five samples taken from the hot spring and cold spring, which served as controls in the study area, were of good quality and accuracy, with ion equilibrium ranging from -3% to 1% (well below the 5% limit) (Table 2). These five samples are suitable for further analysis related to advanced geochemistry, such as determining fluid types, geoindicators, and reservoir geothermometer calculations (Nicholson,1993 ; Powell and Cumming, 2010).

Determination of Water Type ($Cl-SO_4-HCO_3$ Ternary Diagram)

Based on the results of the calculation of the three anion elements that have been presented ($Cl-SO_4-HCO_3$) for five samples (four hot springs and one cold spring) in the Tehoru research area, the results show that HCO_3 content is more dominant than Cl and SO_4 content. The five samples had HCO_3 contents ranging from 74-84%, Cl contents ranging from 8-15%, and SO_4 contents ranging from 7-10%. Based on the calculations in (Table 4), the geothermal fluid type in the Tehoru area is classified into one main group, namely the bicarbonate fluid type, due to the very dominant HCO_3 content compared to the Cl and SO_4 content.

Table 4. Presentation Values of $Cl-SO_4-HCO_3$

Sample Code	Concentration in Parts per Million (mg/L)			Presentation (%)		
	Cl	SO_4	HCO_3	Cl	SO_4	HCO_3
APTHR-1	449.932	292,316	2205,1	15.3%	9.9%	74.8%
APTHR-2	452,642	288,535	2211,1	15.3%	9.8 %	74.9%
APTHR-3	445.393	282,221	2175,1	15.3%	9.7%	74.9%
APTHR-4	103,194	68,311	578,0	13.8%	9.1%	77.1%
ADTHR-1	10,383	8,836	103,6	8.55%	7.2%	84.4%

Based on the plotting results of the three elements $Cl-SO_4-HCO_3$ that have been presented on the (Giggenbach,1988) ternary diagram, the four hot spring samples, namely APTHR-1, APTHR-2, APTHR-3, APTHR-4 and one cold spring ADTHR-1, can be grouped into one main group, classified as bicarbonate water emerging to the surface as peripirial waters (Figure 3). It can be concluded that the four hot springs originate from the same geothermal reservoir.

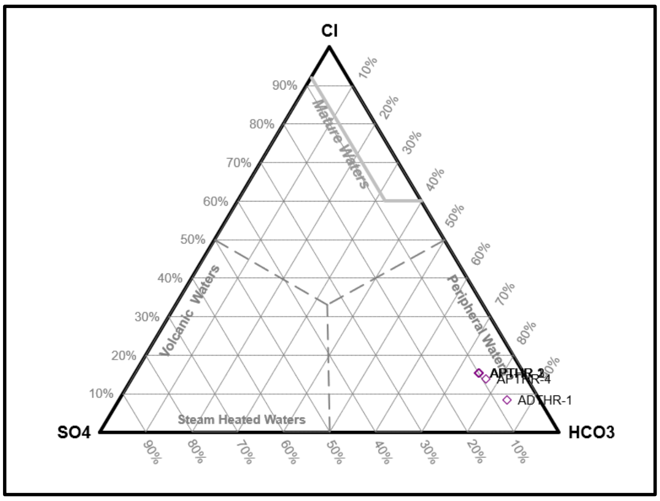

Figure 3. Cl-SO_4-HCO_3 Ternary Anion Plot Illustrating The Proportions of Major

The Bicarbonate water types generally have high chemical HCO_3 content. This type of hot fluid shows the presence of meteoric water heating by a heat source below it or the mixing of fluid from a heat source with meteorite water entering below the surface. The hot fluid undergoes vapor and gas condensation into surface water with an abundance of HCO_3 compared to SO_4 and Cl. This type of fluid usually has a pH close to neutral due to reactions with relatively lateral rocks, and it can be assumed that the three hot springs have reacted with CO_2 or subsurfae water (Lei et al., 2022; Nicholson, 1993). Surface manifestations are usually in the form of warm to hot springs, which can form soda springs, and can be identified by the presence of carbonate sinter deposits around the manifestation site.

Analysis of Dissolved Substances

Based on the results of the calculation of the three anion elements that have been presented (Cl-Li-B), for 5 samples (4 hot springs and 1 cold spring) in the Tehoru research area, the results show that Cl content is more dominant than Li and B content. The five samples had Cl content ranging from 45-48%, Li content ranging from 13-14%, and B content ranging from 37-40%. Based on the above calculations, the geothermal fluid conditions in Tehoru, Central Maluku, are clearly divided into one category for the 5 samples tested (Table 5).

Table 5. Presentation Value of Cl-Li-B

Sample Code	Concentration in Paets per Million (mg/L)			Presentation (%)		
	Cl	Li	B	Cl	Li	B
APTHR-1	449.932	1,360	13,838	48.282%	14.6%	37.1%
APTHR-2	452,642	1,400	15,845	45.778%	14.2%	40.1%
APTHR-3	445.393	1,320	15,018	46.744%	13.9%	39.4%
APTHR-4	103,194	0,335	3,52	45.921%	14.9%	39.2%
ADTHR-1	10,383	0,030	0,344	47.232%	13.6%	39.1%

Of the five samples of hot springs and cold springs, each had different concentrations of each element, but the differences in percentage (%) were not significant. This condition occurred because each geothermal manifestation experienced water–rock interaction during its migration to the surface, and the lithologies traversed by the fluids were relatively similar, resulting in comparable geochemical characteristics (Nicholson, 1993). In addition, the close spatial distribution of the manifestations suggests that they are likely connected to the same hydrothermal system, resulting in comparable geochemical characteristics.

The results of plotting the Cl, Li, and B content (Giggenbach, 1988) show that the four hot springs and one cold spring sample are located in the middle of the Cl, Li, and B triangle diagram, which can also be grouped into one main group (Figure 4). The ratio of Cl and B elements is relatively balanced. The low Li content is due to Li being easily absorbed by secondary minerals such as chlorite, quartz, and clay as a result of reactions with the surrounding rocks that the fluid passes through as it moves to the surface. During its journey, it experiences slight dilution or a decrease in the concentration of dissolved gases and vapors by the rocks through which the hot water flows. The further the fluid migrates to the surface, the more the Li concentration decreases (Nicholson, 1993).

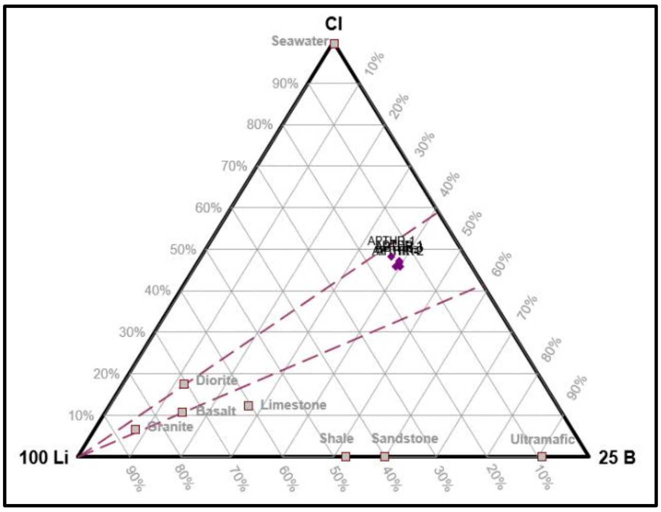

Figure 4. Cl-Li-B (Tclb) Ternary Plot Revealing the Source of the Fluids (Giggenbach, 1991a,b)

The high concentration of B compared to Li also indicates that the geothermal fluid flow moves laterally or sideways before reaching the surface (Nicholson, 1993). Given the location of the hot springs relatively close to the coast, the abundance of Cl compared to Li and B indicates that the four hot springs (APTHR-1, APTHR-2, APTHR-3, and APTHR-4) are located in the outflow zone, indicating these hot springs are shallow groundwater (meteoric water) contaminated by seawater. This can be interpreted as the existence of hot springs from a non-volcanic geothermal system.

Water Maturity Analysis

Based on the calculation results of the three cation elements and several other elements that have been presented (Na-K-Mg), for 5 samples (4 hot springs) and (1 cold spring) in the Tehoru research area, the results show that Mg content is more dominant than Na and K content, but samples APTHR-2 and APTHR-3 have higher Na content compared to the other three samples. The five samples have Na content ranging from 2-12% and 39-58%. K content ranges from 1-7% and 18-28% for Mg content, which is slightly different in 3 groups, with percentages ranging from 13-26%, 42% and 80-96%. Based on the above calculations, the geothermal fluid conditions in Tehoru, Central Maluku, are divided into three clear categories for the five samples tested (Table 6).

Table 6. Presentation Values of Na-K-Mg

Sample Code	Concentration in Paets per Million (mg/L)			Presentation (%)		
	Na	K	Mg	Na	K	Mg
APTHR-1	1248.458	59.480	1.80	39.1992%	18.67563%	42.125%
APTHR-2	1241.373	59.710	0.080	58.519%	28.1476%	13.3333%
APTHR-3	1186.470	61.840	0.440	48.0703%	25.0547%	26.874%

APTHR-4	288.989	17.320	3.750	12.047%	7.22%	80.931533%
ADTHR-1	35.927	2.313	2.738	2.0964%	1.34%	96.553926%

Fluid maturity was analyzed using the Giggenbach (1988) Na-K-Mg ternary diagram, which was chosen for its sensitivity to meteoric water contamination and fluid-rock equilibrium. Based on the evaluation of fluid maturity using the (Giggenbach, 1988) Na-K-Mg ternary diagram. After determining the values of the three Na-K-Mg contents, the percentages of the three elements were calculated and then plotted on the Na-K-Mg ternary diagram. The following are the results of the percentage plotting on the Na-K-Mg ternary diagram by (Giggenbach, 1988) (Figure 5).

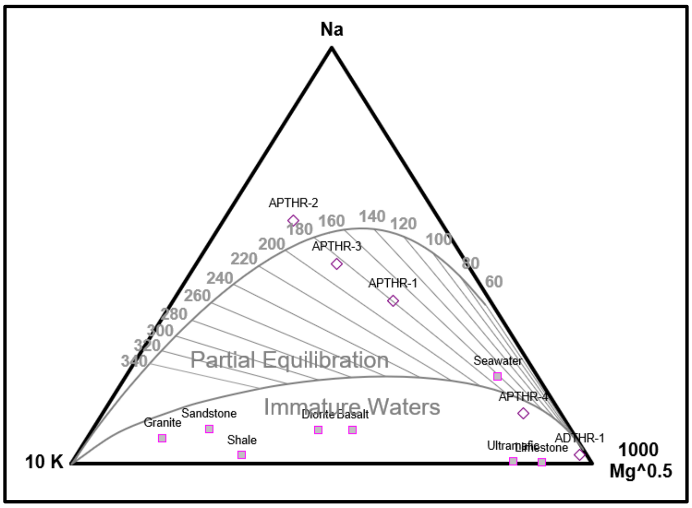

Figure 5. Graphical Evaluation Of The Water-Rock Equilibration Temperatures (Giggenbach, 1988) using Relative Na, K and Mg

Based on the results of plotting the percentages of the three Na-K-Mg contents, it can be seen in the figure above that the APTHR 2 test sample is classified as Full Equilibration, as indicated by the very low percentage of magnesium (Mg) concentration and the dominance of sodium (Na) and potassium (K). This pattern indicates perfect equilibrium between the fluid and the reservoir rock, reflecting circulation in a mature hydrothermal system without significant meteoric water contamination, However, the interpretation of complete equilibration and the absence of meteoric water influence should be treated cautiously, since the Na–K–Mg system remains sensitive to dilution and mixing processes during fluid ascent. Meanwhile, test samples APTHR 1 and APTHR 3 are in a state of "partial equilibrium" with an estimated temperature of 170-180°C. while samples APTHR-4 and ADTHR-1 fall into the immature waters condition. This is evidenced by the relatively high measured Mg content and the imbalance in cation composition (Na/K/Mg is not proportional). The Mg concentration, which is higher than the ideal reservoir limit (0.001–0.1 ppm), indicates the mixing of geothermal fluids with meteoric water that dissolves Mg-rich metamorphic rocks during migration to the surface. APTHR-4 is also likely to be further away from its geothermal reservoir and undergo a more intense mixing process by cold water or meteoric water, resulting in Mg enrichment. Nevertheless, most of the Tehoru hot spring samples tend to plot near the partial equilibrium field, particularly samples APTHR-2 and APTHR-4, which are positioned very close to the partial equilibrium boundary on the Giggenbach Na–K–Mg ternary diagram. This distribution indicates that the geothermal fluids have undergone moderate to advanced water–rock interaction, although complete chemical equilibration with the reservoir rocks may not yet have been fully attained

The Origin of Fluids

The composition of $\delta^{18}O$ and $\delta^{2}H$ isotopes found in geothermal fluids can be used to determine the origin of these geothermal fluids (Zhao et al., 2018). The following are the results of stable isotope $\delta^{18}O$ and $\delta^{2}H$. Stable isotopes ($\delta^{18}O$ and $\delta^{2}H$) were analysed at the Center for Coal and Geothermal Resources Laboratory. Both laboratories are part of the Ministry of Energy and Mineral Resources of the Republic of Indonesia. (Table 7).

Table 7. Laboratory Analysis Results of Isotope

Sample Code	$\delta^{18}O$ (‰)	$\delta^{2}H$ (‰)
APTHR-1	-3,928	-23,992
APTHR-2	-4,021	-23,912
APTHR-3	-4,132	-24,578
APTHR-4	-5,619	-29,470
ADTHR-1	-6,260	-33,816

Based on the isotope analysis data, which was then plotted on a Craig diagram with content parameters ($\delta^{18}O$ and $\delta^{2}H$), it was found that the four hot spring samples and one cold spring sample were located close to the meteoric water line (Figure. 6). This indicates that the five fluids originate from meteoric water that has reacted with low-to-moderate temperature surrounding rocks before reaching the surface. However, the reaction between the fluid and the rocks can be said to be not very intense because the oxygen $\delta^{18}O$ content is still below 3.5 (Nicholson, 1993). The reaction between the geothermal fluid and the rock causes oxygen transfer from the rock to the fluid. The effect of evaporation is not intense, having minimal impact on isotope enrichment, and is thought to be predominantly the result of rock mineral exchange processes.

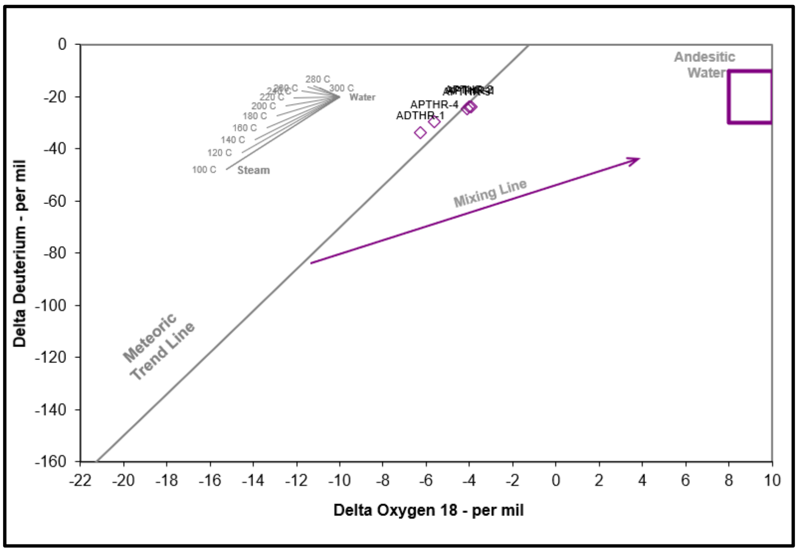

Figure 6. Isotope $\delta^{18}O$ and $\delta^{2}H$ Graphic in the Study Area for 5 Samples (Craig, 1961).

The results of stable isotope analysis ($\delta^{18}O$ and $\delta^{2}H$) show that all geothermal fluid samples in the Tehoru region originate from meteoric water that has seeped into the ground. All of the hot water has undergone slight enrichment in oxygen-18 and deuterium, indicating interaction between the hot fluid and the rock. Isotope values close to the global meteoric water line (GMWL), especially those touching the line, indicate the absence of magmatic fluid or seawater influence, as supported by the cation–anion composition, especially the relatively low concentrations of lithium (Li) and chloride (Cl). A small shift in $\delta^{18}O$ towards the positive, especially in samples APTHR-1, APTHR-2, and APTHR-3, indicates water-rock isotope exchange at high temperatures (oxygen shifting) and greater depths. The more negative $\delta^{18}O$ isotope values in samples APTHR-4 and ADTHR-1 are due to mixing with shallow water. These findings confirm that the Tehoru geothermal system is a non-volcanic system with deep meteoric water circulation (Giggenbach, 1992).

Shoeller Diagram

The following are the results of the main ion concentration values (in mg/L) converted into base 10 logarithms (log C) (Table 8). The main ions are then plotted sequentially on the horizontal axis, while the vertical axis uses a logarithmic scale to show the concentration (usually in meq/L or mg/L) (Shah, 2021).

Table 8. Results of Main Ion Concentrations to be included in (Scholler, 1965)

Sample Code	Li	Na	K	Mg	Ca	F	Cl	HCO_3	SO_4	B	NH_4
APTHR-1	0,13	3,10	1,77	0,26	0,48	0,72	2,65	3,34	2,47	1,14	0,90
APTHR-2	0,15	3,09	1,78	-1,10	0,30	0,72	2,66	3,34	2,46	1,20	0,84
APTHR-3	0,12	3,07	1,79	-0,36	0,28	0,71	2,65	3,34	2,45	1,18	0,87
APTHR-4	-0,47	2,46	1,24	0,57	1,20	0,20	2,01	2,76	1,83	0,55	0,35
ADTHR-1	-1,52	1,56	0,36	0,44	0,66	-0,72	1,02	2,02	0,95	-0,46	-2,00

Based on the plotted results, it can be inferred that the Tehoru hot spring water samples APTHR-1, APTHR-2, and APTHR-3 exhibit similar cation concentrations, with the relative abundance of cations in each sample following the order Na > K > Ca > Mg (meq/L). Samples APTHR-1, APTHR-2, and APTHR-3 also display nearly identical anion concentrations. The overall anion abundance for all samples follows the sequence HCO_3 > Cl > SO_4.

In general, all samples show a pattern of bicarbonate (HCO_3) and sodium (Na) ion dominance, where these two ions have the highest log concentration values compared to other ions. This indicates that the hot water in Tehoru belongs to the Na–HCO_3 type, which is characteristic of medium to deep geothermal fluids that have interacted strongly with reservoir rocks (Lv et al., 2023). The high presence of Na^+ ions can also be caused by the dissolution of silicate minerals (such as feldspar and plagioclase) and cation exchange, where Ca ions from rocks are exchanged with Na^+ in fluids (Gao et al., 2023). The concentration patterns of the four hot springs are higher than those of cold water, except for some chemical elements such as Mg and Ca, which are indeed more dominant in cold water (Figure 7).

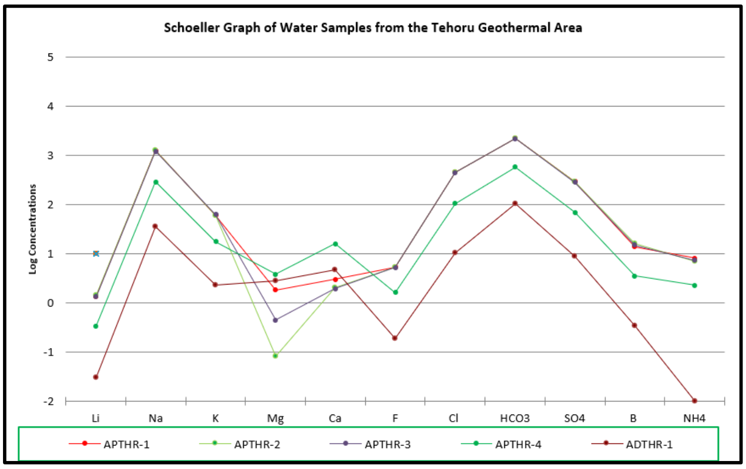

Figure 7. Schollers Plot Showing Concentrations of Various Cations and Anions in Four Different Samples in the Study Area.

HCO_3 ions (bicarbonate) showed high values in all five samples, indicating the dissolution of carbonate minerals ($CaCO_3$ and dolomite) along the hot water flow path. This high HCO_3 content indicates the influence of meteoric water (rainwater that seeps into the ground) mixing with deep hot water, this is supported by the results of stable isotope analysis of four hot spring water samples and one cold spring water sample from the

study area. This process commonly occurs in non-volcanic or mixed geothermal systems, where rainwater is heated through contact with hot rocks below the surface before reemerging as hot springs (Li et al., 2021).
In addition, SO_4 (sulfate) concentrations were also relatively high in several samples, particularly APTHR-1, APTHR-2, and APTHR-3. High SO_4 content may originate from the oxidation of H_2S gas to sulfate or from the dissolution of sulfate minerals such as gypsum and anhydrite. This indicates that some of the hot water may have been mixed with shallow or immature water, which has interacted with the oxidative environment near the surface (Yuan et al., 2024; Giggenbach, 1991 & 1989). Minor ions such as Li, K, F, ⁻, and NH_4 show relatively low concentrations in all samples. The low levels of these elements indicate that the Tehoru geothermal system does not show significant influence from magmatic fluids, but is instead influenced by meteoric water heated by the non-volcanic geothermal system heat gradient (Dávalos-Elizondo et al., 2021; Wrage et al., 2017).

Estimation of Subsurface Temperature

To estimate the temperature of geothermal reservoirs, dissolved geothermometers such as cations are used. Temperature estimates obtained from the four Tehoru hot spring samples (Table 9). Geothermometers are one method for estimating reservoir temperature based on the presence of dissolved substances in hydrothermal fluids (Ariwibowo, 2012). The best samples for geothermometers are chloride waters with high temperatures and discharge rates (>60°C and ≥2 L/second; (Nicholson, 1993).

Table 9. Temperature Obtained From Geochemical Analysis Results

Sample Code	Na-K (Fournier,1979)	Na-K (Giggenbach,1988)
APTHR-1	161	179
APTHR-2	161	180
APTHR-3	167	185
APTHR-4	177	194

Based on geothermometers from the four hot springs (Table 8), the reservoir temperature in the study area ranges from 161 to 194°C (Giggenbach, 1988; Fournier 1979). From the geothermometer calculations of these hot springs, it can be said that the Tehoru geothermal area is classified as a medium-temperature geothermal system (Hochstein, 2008).

Conclusions

Based on the results of geochemical and fluid isotope analysis of the five samples. The main results obtained are that the hydrothermal fluid in the Tehoru Geothermal System originates from heated meteoric water infiltration because it has HCO_3 content and appears as peripheral springs in lateral outflow. The high percentages of Cl and B indicate that the four hot water samples are water from reservoirs that have traveled a considerable distance and undergone intense interaction between the fluid and the rock, as illustrated by the decreasing B content relative to Li. There are three categories of geothermal fluid equilibrium in the study area, including APTHR-2 Fullequilibrium, APTHR-1 and APTHR-3 Partial Equilibrium, and APTHR-4 and ADTHR-1, which are Imaature Water. This result is supported by the data from the stable isotope analysis $\delta^{18}O$ and $\delta^{2}H$ because the four hot spring samples are on the global meteoric water line (GMWL). Based on the estimated reservoir temperature calculations for the Tehoru Geothermal System (161-194°C), which is classified as a medium-enthalpy geothermal system (Hochstein, 2008).The Tehoru geothermal system is not directly related to active volcanic activity, thus falling under the category of non-volcanic geothermal potential in Indonesia. This is supported by the lithological conditions in the study area, which consists of metamorphic and altered rocks, further strengthening the results of previous studies and confirming that there is indeed no volcanic activity in the Tehoru Geothermal Area, Maluku, Indonesia. The type of geothermal system in Tehoru is likely a fractured system or a heat sweep system, but this still requires additional geophysical data.

Acknowledgment

We would like to express our deepest gratitude to the Faculty of Geological Engineering, Padjadjaran University, and the Education Fund Management Institution (LPDP) of the Ministry of Finance of the Republic of Indonesia for their assistance in financing and analyzing the laboratory so that this research could be carried out properly.

References

Aribowo. Y. (2012). Prediksi Temperatur Reservoar Panasbumi Dengan Menggunakan Metoda Geotermometer Fluida Prediksi . TEKNIK, vol. 32, no. 3, pp. 234-238, Feb. 2012. https://doi.org/10.14710/teknik.v32i3.1743 (In Bahasa Indonesia).

Arnorsson, S., Gunnlaugsson, E., & Svavarsson, H. (1983). The chemistry of geothermal waters in Iceland. III. Chemical Geothermometry in geothermal investigations. Geochim. Cosmochim. Acta 47, 567-577.

Arrofi, D., Abu-Mahfouz, I. S., & Prayudi, S. D. (2022). Investigating high-permeable zones in non-volcanic geothermal systems using lineament analysis and fault fracture density (FFD): northern Konawe Regency, Indonesia. Geothermal Energy, 10(1). https://doi.org/10.1186/s40517-022-00241-3

Appelo, C.A.J & Postma, D. (2005), Geochemistry, Groundwater and Pollution, Second Edition: Boca Raton, CRC Press, 125-129

Carter,D.j.Audley-Charles,M.G & Barber,A.J. (1976) Stratigraphic Analysis of Island Arc Continental Margin Collision in eastrn indonesia J.Geol.SOc.London,N/v132, 79-198

Craig, H., (1961). Isotopic Variations in Meteoric Waters. Science, 133(3465), 1702-1703.

Dávalos-Elizondo, E., Atekwana, E. A., Atekwana, E. A., Tsokonombwe, G., & Laó-Dávila, D. A. (2021). Medium to Low Enthalpy Geothermal Reservoirs Estimated From Geothermometry and Mixing Models of Hot Springs Along the Malawi Rift Zone. Geothermics, 89. https://doi.org/10.1016/j.geothermics.2020.101963

Directorate of Geothermal Energy, Ministry of Energy, Directorate General of EBTKE and Center for Mineral, Coal and Geothermal Resources, Indonesian Geological Agency (2017). Indonesia's Geothermal Energy Potential Volume 2 :Jakarta , 722-725

D'Amore, F., Arnorsson, S.,(2000). Geothermometry. In: Arnorsson, S. (Ed.), Isotopic and Chemical Techniques in Geothermal Exploration, Develop ment and Use. International Atomic Agency, Vienna, 152-199.

Fahira, G. H., Sukiyah, E., & Muslim, D. (2025). Quantitative Geomorphology Approach in the Assessment of Relative Tectonic Activity in Cikandang Watershed. 20(1), 22–35.

Fink, J., Heim, E., & Klitzsch, N..(2021). State of the Art in Deep Geothermal Energy in Europe with Focus on Direct Heating SpringerBriefs in Earth System Sciences. (https://link.springer.com/bookseries/10032)

Fournier, R.O., & Rowe, J.J. (1977). Estimation of Underground Temperatures from The Silica Content of Water from Hot Springs and Wet-steam Wells. American Journal of Science, 264.

Fournier, R.O., (1979). A revised equation for the Na/K geothermometer. GRC Transactions, 3, 221-224.

Gao, Z., Hao, M., Liu, J., Li, Q., Tan, M., & Niu, Y. (2023). A Comprehensive Study on the Hydrogeochemical and Isotope Characteristics and Genetic Mechanism of Geothermal Water in the Northern Jinan Region. Energies, 16 (22). https://doi.org/10.3390/en16227658

Giggenbach, W.F., (1988). Geothermal Solute Equilibria. Derivation of Na-K-Mg-Ca Geoindicators. Geochimica et Cosmochimica Acta, 52(12), 2749-2765.

Giggenbach, W.F., (1991). Chemical Techniques in Geothermal Exploration. Application of Geochemistry in Geothermal Reservoir Development, 119-144.

Giggenbach, W. F. (1992). Isotopic shifts in waters from geothermal and volcanic systems along convergent plate boundaries and their origin. In Earth and Planetary Science Letters. Vol. 113.

Giggenbach, W.F. (1989). The Chemical and Isotopic Position of The Ohaaki Field Within The Taupo Volcanic Zone. Proc. N.Z. Geothermal Workshop 11, 81–88

Hochstein, M.P. & Sudarman, S., (2008). History Of Geothermal Exploration in Indonesia From 1970 to 2000. Geothermics, 37(3), 220-266.

Hochstein, M.P., & Browne, P.R.L. (2000). Surface Manifestation of Geohtermal System with Volcanic Heat Sources, in Encyclopedia of Volcanoes.

Koesoemadinata, R. P. (2025). An introduction into the geology of Indonesia: Volume II, Part 2 Central Indonesia and Part 3 Eastern Indonesia. ITB Press

Kumalasari, D. I., Kusuma, A. G., Mahalka, H., Syarifatullah, M. S., & Gumelar, N. A. (2020). Geochemical Prospecting Investigation in Non-Volcanic Geothermal Area: A Case Study of Sajau, East Tanjung Palas, Bulungan, North Kalimantan. IOP Conference Series: Earth and Environmental Science, 417(1). https://doi.org/10.1088/1755-1315/417/1/012004 (In Bahasa Indonesia).

Lei, Y., Zhao, Z., Zhang, B., Tang, X., Luo, Y., Wang, G., Gao, J., & Zhang, D. (2022). Genesis of Significance of Carbonated Thermal Water Springs in Xining Basin, China. Water (Switzerland), 14(24). https://doi.org/10.3390/w14244058

Li, X., Qi, J., Yi, L., Xu, M., Zhang, X., Zhang, Q., & Tang, Y. (2021). Hydrochemical Characteristics and Evolution of Geothermal Waters in The Eastern Himalayan Syntaxis Geothermal Field, Southern Tibet. Geothermics, 97. https://doi.org/10.1016/j.geothermics.2021.102233

Lv, G., Zhang, X., Wei, D., Yu, Z., Yuan, X., Sun, M., Kong, X., & Zhang, Y. (2023). Water–Rock Interactions, Genesis Mechanism, and Mineral Scaling of Geothermal Waters in Northwestern Sichuan, SW China. Water (Switzerland), 15(21). https://doi.org/10.3390/w15213730

Mulki, D., Dwi, H., Sunuhadi, N., Dedi, A., Herry, M., R. E., Daya, N.S., Batubara, C., Metana, G., Arya, B., Sigit, J., Wibisono, A., Abdurahman, M., Penny, I., Rahmat, O., Fatimah, H., Neraca, P., Daya, S., Panas, C., & Taufik, A. . (2021). Penyusun Neraca Sumber Daya dan Cadangan Mineral Batubara dan panas bumi Indonesia 2021; Jakarta (In Bahasa Indonesia).

Ministry of Energy and Mineral Resources of Indonesia, (2019). Sistem panas bumi non-vulkanik Indonesia. https://geologi.esdm.go.id/media-center/sistem-panas-bumi-non-vulkanik-di-indonesia , (accessed 1st January 2026)

Murillo, R.S, Brooks, E.S., Elliot, W.J. &Boll, J., (2015). Isotope hydrology and baseflow geochemistry in natural and human-altered watersheds in the Inland Pacific Northwest, USA. Isotopes in environmental and health studies, 51(2), 231-254.

Nicholson, K. (1993). Geothermal fluids: Chemistry and Exploration Techniques. Springer-Verlag. https://doi.org/10.1007/978-3-642-77844-5

Pinning, F., Haryanto, A. D., & Hutabarat, J. (2023). Hydrogeochemistry and Isotope Characteristics of the Hot Springs in the Wapsalit Area, Buru Regency, Maluku Province, Indonesia. Journal of Geoscience, Engineering, Environment, and Technology, 8(4), 269–274. https://doi.org/10.25299/jgeet.2023.8.4.13788

Powell, T., & Cumming, W. (2010). Spreadsheets for geothermal water and gas chemistry. Geothermal Resource Group.

Rezky, Y., & Zarkasyi, A. (2010). Indication of Intrusive Body in Wapsalit Geothermal Area, Buru Island, Indonesia. World Geothermal Congress. Bali.

Rochayati, N. (2025). Interaksi Tiga Lempeng di Kawasan Indonesia Timur (Vol. 1, Issue 2). https://journal.ummat.ac.id/index.php/ecs (In Bahasa Indonesia).

Santia, O., Mustofa, A., & Hadi, M.N. (2021). Laporan Survei Rinci Geologi Daerah Panas Bumi Cisolok-Cisukarame Kabupaten Sukabumi Provinsi Jawa Barat ; Bandung Indonesia (In Bahasa Indonesia).

Schoeller, H., (1965). Hydrodynamique Dans Lekarst (Ecoulement et emmaga sinement). Actes Collogues Dubrov. I, 3-20.

Syaiful, (2020). Tektonostratigrafi Busur Banda Luar Dengan Referensi Bagian Barat Timor Leste dan Bagian Timur Pulau Seram . Pusat Survei Geologi. https://doi.org/10.33332/jgsm.geologi.v21i2.135 (In Bahasa Indonesia)

Shah, M., Sircar, A., Shah, V., & Dholakia, Y. (2021). Geochemical and Geothermometry Study On Hot-Water Springs For Understanding Prospectivity Of Low Enthalpy Reservoirs of Dholera Geothermal field, Gujarat, India. Solid Earth Sciences, 6(3), 297–312. https://doi.org/10.1016/j.sesci.2021.04.004

Tjokrosapoetro, S., Achadan, A., Rusma, E., Suwitodirjo, K., & Bidin, H.Z. (1993). Regional Lembar Masohi, Maluku Skala 1: 250.000. Pusat Penelitian dan Pengembangan Geologi Lembar 2612, 2613, 2712, 2713.

Verstappen, H. T. (2010). Indonesian Landforms and Plate Tectonics. In Jurnal Geologi Indonesia (Vol. 5, Issue 3).

Wrage, J., Tardani, D., Reich, M., Daniele, L., Arancibia, G., Cembrano, J., Sánchez-Alfaro, P., Morata, D., & Pérez-Moreno, R. (2017). Geochemistry Of Thermal Waters in The Southern Volcanic Zone, Chile – Implications for Structural Controls On Geothermal Fluid Composition. Chemical Geology, 466, 545–561. https://doi.org/10.1016/j.chemgeo.2017.07.004

Yuan, W., Xing, Y., Wei, M., Guo, X., Liu, J., Gao, J., Zhang, C., & Zhai, Y. (2024). Hydrochemical Characteristics and Indication to Geothermal Genesis of Low–Medium-Temperature Convection Geothermal Field in Yanshan Orogenic Basin, China. Water (Switzerland), 16(3). https://doi.org/10.3390/w16030433

Zhao, R., Shan, X., Yi, J., Du, X., Liang, Y., Zhang, Y., (2018). 274 Geochemistry of HCO3-Na thermal Water From The Gudian Slope: Insights Into Fluid Origin, Formation Mechanism and Circulation in The Yitong Basin, Northeast China. Applied Geochemistry 91, 185–196. https://doi.org/10.1016/j.apgeochem.2017.10.014